Conformational behavior of oxygenated mycobacterial mycolic acids from *Mycobacterium bovis* BCG

Masumi Villeneuve[†1] Mizuo Kawai[†] Motoko Watanabe[‡] Yutaka Aoyagi[‡]
Yukio Hitotsuyanagi[‡] Koichi Takeya[‡] Hiroaki Gouda[§] Shuichi Hirono[§]
David E. Minnikin[¶] Hiroo Nakahara[†]

†Department of Chemistry, Faculty of Science, Saitama University
255 Shimo-okubo, Sakura-ku, Saitama, 338-8570 Japan

‡School of Pharmacy, Tokyo University of Pharmacy and Life Science
1432-1 Horinouchi, Hachioji, Tokyo, 192-0392 Japan

§School of Pharmaceutical Sciences, Kitasato University
5-9-1 Shirokane, Minato-ku, Tokyo, 108-8641 Japan

¶School of Biosciences, The University of Birmingham
Edgbaston, Birmingham, B15 2TT UK

[1]corresponding author

Key words *Mycobacterium bovis* BCG; oxygenated mycolic acid; phase diagram; thermodynamics; Langmuir monolayers

Abstract

Phase diagrams of Langmuir monolayers of oxygenated mycolic acids, i.e. methoxy mycolic acid (MeO-MA), ketomycolic acid (Keto-MA), and artificially obtained deoxo-mycolic acid (deoxo-MA) from *Mycobacterium bovis* BCG were obtained by thermodynamic analysis of the surface pressure (π) vs. average molecular area (A) isotherms. At lower temperatures and surface pressures, both Keto- and MeO-MAs formed rigid condensed monolayers where each MA molecule was considered to be in a 4-chain form, in which the three carbon chain segments due to bending of the 3-hydroxy aliphatic carboxylate chain and the 2-side chain were in compact parallel arrangement. At higher temperatures and surface pressures, MeO-MA and deoxo-MA tended to take stretched-out conformations in which the 3-hydroxy aliphatic carboxylate chain was more or less in an extended form, but Keto-MA retained the original 4-chain structure. The thickness measurement of the monolayers *in situ* by ellipsometry at different π values and temperatures supported the above conclusions derived from the phase diagrams. The enthalpy changes associated with the phase transitions of MeO-MA and deoxo-MA implied that the MeO-MA needed larger energy to change from a compact conformation to an extended one, possibly and partly due to the dehydration of the methoxy group from water surface involved. Molecular dynamics studies of MA models derived from Monte Carlo calculations were also performed, which confirmed the conformational behavior of MAs suggested by the thermodynamic studies on the Langmuir monolayers.

1 Introduction

Mycolic acids (MAs), high-molecular-mass 2-alkyl branched, 3-hydroxy fatty acids are characteristic components of the mycobacterial cell envelope, most of which are esterified to cell wall penta-arabinosyl units [1–3]. MA structures have characteristic features, comprising a long saturated 2-alkyl branch and the main so-called "meromycolate" chain. The meromycolate chain of pathogenic mycobacteria normally has two intra-chain functional groups that vary in type, stereochemistry and spacing. Structures of various MAs from representative mycobacteria have been characterized [4, 5].

In the structural models of the mycobacterial cell envelope proposed previously [2, 6], MAs covalently linked to penta-arabinosyl residues of cell wall arabinogalactan are arranged perpendicular to the cell wall, forming a highly structured monolayer. Recent computer simulation work supported such arrangement of MAs as proposed in the model [7]. This outer leaflet of mycobacterial cell envelope is considered to provide the cells with a special permeability barrier responsible for various physiological and pathogenic features of mycobacterial cells [8]. There are various other lipids in the mycobacterial cell envelope and they may also take part in the permeability function of the cell envelope as suggested [2, 6, 9]. Recently, a *Mycobacterium tuberculosis* (*M. tb*) mutant whose MA comprises only alphamycolic acid (α-MA) [10], a recombinant mutant having over-produced methoxymycolic acid (MeO-MA) with no ketomycolic acid (Keto-MA) [11] and a mutant having 40 % less cell wall mycolate [8] have been described. These results show that *M. tb* can be viable with highly modified mycolic acid composition and that its pathogenicity may be related to the types of MAs. Those papers also

suggest that MAs on the cell envelope have determining effect on the permeability barrier function of the cell wall outer hydrophobic layer barrier and different MAs may contribute to the cell wall permeability barrier functions in different ways.

In our previous paper, to simulate the conformational behavior of MAs in the cell envelope mycolate layer, we prepared insoluble monolayers at the air/water interface (Langmuir monolayers) of α-, MeO-, and Keto-MAs from *M. tb* and studied their phase diagrams by thermodynamic analysis [12]. The results implied that at low temperature (T) and surface pressure (π), all these MAs might assume a condensed four-chain structure in which the 2-alkyl side chain and the three methylene-chain segments are parallel to each other (Figs. 1a and b). The two functional groups appear to allow the meromycolate chain to fold up into this compact parallel arrangement. As T and π are increased, α- and MeO-MAs tend to take stretched-out structures in which the distal functional group in the meromycolate chain leaves the near-hydroxy group location (Fig. 1c). The conformation of Keto-MA is little affected by the changes in T and π and the four-chain form is retained.

In the present study, we made detailed analysis of Langmuir monolayers of oxygenated MeO- and Keto-MAs from *Mycobacterium bovis* BCG (BCG) and deoxo-MA, prepared from Keto-MA by reduction, and studied their phase diagrams. MeO-MA and Keto-MA from BCG have much lower *trans*-cyclopropane ring content [4,5] than those from *M. tb*, so light may be shed on the effect of the *trans*-cyclopropane group on the conformation of oxygenated mycolates. The thickness of the Langmuir monolayers was also analyzed at different T and π *in situ* by ellipsometry, a technique for characterization

of thin films by introducing polarized light on to the film and analyzing the changes in the reflected light. Computer simulation of the conformational changes of those MAs was also performed, using Monte Carlo (MC) calculations and molecular dynamics (MD) simulations. All these results obtained by different approaches agreed with the estimation of conformation features of MAs shown by the phase diagram analysis.

2 Materials and Methods

Materials used: The samples used in the present experiment were type-1 MeO- and Keto-MAs from *Mycobacterium bovis* BCG strain Tokyo 172, prepared as described previously [4,5] and an artificially prepared deoxo-MA obtained by reduction of Keto-MA. The structural characteristics, compositions and average molecular weights of the MAs studied are summarized in Table 1.

Preparation of deoxo-mycolic acid: Keto-MA from BCG (200 mg, 0.16 mmol ca.) was dissolved in a 4 : 1 (v/v) mixture of benzene-methanol (5.0 ml) under argon. After addition of tosylhydrazine (50 mg, 0.27 mmol), the solution was stirred at 80 °C for 3 hr. The solvent was removed under reduced pressure and the residue was dissolved in sulfolane (2.5 ml) under argon. After addition of tosic acid (5.0 mg) and sodium cyanoborohydride (50 mg, 0.8 mmol), the solution was stirred at 100 °C for 12 hr. The reaction mixture was diluted with diethyl ether, washed with saturated aqueous sodium chloride solution, dried over magnesium sulfate and evaporated under reduced pressure to give crude deoxo-MA, which was purified by silica

gel TLC using diethyl ether-hexane (1 : 4 v/v), giving a 30 % yield.

Other reagents: Distilled reagent grade chloroform (Wako chemicals) was used as the spreading medium. Water was distilled once and deionized by Milli-Q Plus (resistance 18.2 MΩ cm).

π vs. A isotherms measurement: The Langmuir monolayer was prepared by spreading a chloroform solution of MA (1 ml, ca. 6×10^{-5} M) on the water surface. Surface pressure (π) vs. mean molecular area (A) isotherms of the Langmuir monolayer of MA spread on water were measured by a Lauda film balance (FW1). The area of the water surface was about 562 cm^2 in this trough. The compression rate of the monolayer was 14 $Å^2$ $molecule^{-1}$ min^{-1}. π vs. A isotherms were measured at intervals of 2 °C in the range of $10 \sim 46$ °C. The subphase temperature was controlled within the accuracy of ±0.2 °C. The room temperature was thermostatted at 23 ± 1 °C.

Ellipsometry: Ellipsometry was performed on a Nanofilm EP^3 (NFT Co., Göttingen, Germany) with a home-built trough installed on the stage. The trough was thermostatted at the temperatures as specified in Table 2 (error within ± 0.2 °C). The monolayer was prepared and compressed with a Teflon-coated barrier to the target π values. The refractive index was taken to be 1.48 in evaluation of monolayer thickness.

Computer simulation of the conformation of mycolic acid: MC calculations: The software used for this calculation was MacroModel ver. 6.0 (Schrödinger Inc., Portland, Oregon, USA). The MAs subjected to these calculations were *cis*-cyclopropyl MeO-MA with $n-m-l$ of 17−16−17, *trans*-cyclopropyl MeO-MA with $n-m-l$ of 18−16−17, *cis*-cyclopropyl Keto-MA with $n-m-l$ of 15−18−17 and 17−18−17 and *trans*-cyclopropyl Keto-MA

with $n-m-l$ of $16-18-17$ (Table 1). Deoxo-MA was assumed to have the same component ratio and $n-m-l$ values as the parent Keto-MA. The starting general structure prepared for MC computation was as shown in Fig. 2a. In the Figure, [X] is -CH(CH_3)-CH(OCH_3)- or -CH(CH_3)-CO-, where both of the asymmetric carbons are *S* in the former [15], and the asymmetric carbon in the latter made *S*. [Y] is either *cis*- or *trans*-cyclopropane with an adjacent methyl group in the case of *trans*-cyclopropane. In those structure models, the distal and the proximal carbons of *cis*-cyclopropane were made *S* and *R*, respectively, and those of *trans*-cyclopropane *S* and *R*, respectively, with the adjacent methyl-bearing carbon made *S*. [Z] is -CH_2-C2H(COOH)-C3H(OH)-CH_2-. The absolute configurations at C2 and C3 are both *R*, the interrelation of the two centres thereby being erythro. In [Z], the NMR proton coupling constant between the hydrogens attached to C2 and C3 of MAs of this series is average 9.0 Hz. Calculation of the dihedral angle, H-C2-C3-H, by using the approximated formula by Pachler [16] and by the further modified formula by Haasnoot et al. [17] gave a set of dihedral angles of approximately $+160 \sim 161$ ° and $-148 \sim -146$ °. The latter formula gave also another set of angles producing near ecliptic conformations, which are not likely and these were not considered. Accordingly, the carbon dihedral angle in [Z] involving C2, C3 and the adjacent carbons to each were considered to be either $40 \sim 41$ °, or $92 \sim 94$ °. The model structures for MC were made accordingly, in which the carbon dihedral angles were 40, 41, 92, 93 or 94 °. Intra-molecular hydrogen bonding was assumed to exist between 3-hydroxy group and the carboxyl group, and thus, the distance between the hydrogen of the 3-hydroxyl group and the carbonyl oxygen of the carboxyl groups was

restricted to be in the range of 2.4 ± 0.6 Å. In Figure 2a, the fat line portions are aliphatic carbon chain segments, made to straight chain segments for quicker calculations (dihedral angles = 180 °) in the MeO- and Keto-MAs. Three carbons on both sides adjacent to the intra-chain functional groups [X] and [Y], and 2 carbons on both sides adjacent to [Z] in the methylene chains were not included in the restriction segments. In the case of deoxo-MA, this chain-straight-up restriction was not applied to the meromycolate chain. The structural models of the MAs with the restrictions specified above were subjected to MC. The strength of the restriction force for the dihedral angles was 100 kcal rad^{-2} constant force and for the range 200 kcal Å^{-2} constant force. Some models were subjected to MC at different force strength on the torsion angle restrictions, i.e. 90 or 110 kcal rad^{-2}, to obtain two or three different structures for MD. The force field used was MM2*. The length of the calculation was 15000 iterations.

MD simulations: The MA models produced by MC calculations were subjected to energy minimization, by the gradient system with the minimum energy change of 0.05 kcal mol^{-1}, by using the software sybyl6.91 (Tripos) with the force field MMFF94. Restrictions were applied only to the above specified carbon dihedral angle in [Z] and to the range of the distance between the hydrogen of 3-hydroxyl group and the carbonyl oxygen of the carboxyl group ($1.8 - 3.0$ Å) as specified for MC calculations, with the force constant of 5.0 kcal rad^{-2} and 200 kcal Å^{-2}, respectively. Most of them reached their final minimization stages before 500 iterations. Since even subtle differences in the starting conformation affect the MD results, for each, $3 - 5$ models were chosen at 50 iteration intervals between the final minimization stage

iteration and 200th iterations, and each was subjected to MD simulation with the temperature set at 320 K. The software, the force field and the restrictions applied in MD were all as for the minimization. The length was 20 ps (2 ps $\times$10).

Grouping of conformations resulting from MD simulation: For evaluation of the structures resulting from MD simulation of the models derived from MC calculations, the following 5 points were chosen, as illustrated in Figure 2b: the first carbon of the carboxylate chain (a), C2 (b), the distal carbon of the cyclopropane ring (c), methoxy- or oxo-group-bearing carbon or the methylene carbon produced by removal of the oxo group (d) and the distal end carbon of the meromycolate chain (e). According to the distances between them, the resulting structures were grouped as follows. When the distances a/b, b/c, c/d and d/e were all above 70 % of the original lengths, the spacing a/c, a/e and c/e all less than twice the original values and b/d less than 18 Å, the resulting structure was taken as "4-chain structure (A in Table 3. See Figs. 1a and b). When the above requirements as to the distances a/b, b/c, c/d, d/e, a/c, c/e and a/e were satisfied and the spacing b/d was between 18 to 22 Å, the structure was grouped into "In-between structure" (A/B in Table 3). When a/b and b/c were both above 70 % of the original lengths, with b/d above 23 Å, and a/c less than twice the original value, the structure was defined as "Stretched-out structure" (B in Table 3. See Fig. 1c). When the resulting structures could not be grouped into any of the three groups defined above, they were placed under "Non-definable structures". They normally included the structures having the a/b and/or d/e chains with serious mid-chain bent or stretching out into wrong

directions.

3 Results

3.1 Phase diagrams of Langmuir monolayers of the MAs

The π vs. A isotherms of MeO-MA, Keto-MA and deoxo-MA are shown in Figs. 3a, b and c, respectively. The phase diagrams for them were constructed by plotting the surface pressures at the bends on the π vs. A isotherms which correspond to the phase transitions π^{tr} and to film collapsing π^{cp} against the temperature and shown in Fig. 4. The state of each phase was characterized by estimating the elasticity modulus of the monolayer, which is defined by $E = -A(\partial\pi/\partial A)_{T,p}$ as done in our previous work [12]. LE, LC and SC refer to the liquid expanded, liquid condensed and solid condensed films, respectively. Fig. 5 illustrates A^{tr}, the mean molecular areas at π^{tr} or A^{cp} that at collapse surface pressure vs. T curves for each MA. Detailed studies on the mean molecular area in reference to information provided by the elasticity modulus of the Langmuir monolayer gives us an insight into molecular conformation at the air/water interface.

As seen in Fig. 4a, MeO-MA from BCG exhibited a range of phases and a characteristic phase transition of which surface pressure greatly decreased with an increase in temperature. This phase transition has been confirmed to be reversible by repeated compression-expansion measurement of the π vs. A isotherm. The monolayer took two different condensed states in the

two phases separated by this boundary. A^{tr} takes values from 80 to 120 Å^2 molecule^{-1}. Especially, below 32 °C MeO-MA monolayer is in a condensed state at the surface pressures below π^{tr} as suggested by e.g., $E = 250$ mN m^{-1} at $\pi = 20$ mN m^{-1} and $T = 18$ °C or $E = 150$ mN m^{-1} at $\pi = 8$ mN m^{-1} and $T = 24$ °C. On the other hand, A^{cp} takes values less than 70 Å^2 molecule^{-1}. The phase transition observed around $\pi \simeq 19$ mN m^{-1} from $T = 10$ to 18 °C is a transition from a four-chain conformation to another four-chain conformation with different molecular packing states as suggested by $A^{\mathrm{tr}} \sim 85$ Å^2 molecule^{-1} shown in Fig. 5a.

The π vs. A isotherms of all the MAs showed complex dependence on temperature however, the phase diagram of Keto-MA shown in Fig. 4b is much simpler than that of MeO-MA. Keto-MA forms a condensed monolayer more rigid than a liquid condensed film but less stiff than a solid condensed film over a wide rage of temperature and surface pressure. A^{cp} of Keto-MA is shown to be slightly higher than 80 Å^2 molecule^{-1}. Moreover, the monolayer is in a condensed state, i.e., $E = 260$ mN m^{-1} at $\pi = 20$ mN m^{-1} and $T = 32$ °C. Accordingly, it seems reasonable to assume that in the Keto-MA molecules the meromycolate chain bends at the cyclopropane and at the carbonyl group to form a 4-chain structure whose four hydrocarbons are packed tightly in parallel, with the carbonyl group touching the water surface and hydrated.

Therefore, it is suggested that MeO-MA molecules take a conformation similar to that of Keto-MA in the low surface tension and low temperature region of the phase diagram and at surface pressures above π^{tr}, they are aligned with the meromycolate chain detached from the water surface.

As shown in Fig. 4c, deoxo-MA prepared by deoxygenation of Keto-MA gave a completely different phase diagram from that of the original Keto-MA. The apparently stable monolayers observed in the π vs. A isotherms of deoxo-MA, in the region above LC III and LE, were concluded, by analysis of the repeated compression-expansion isotherms, to be collapsed films.

3.2 Thickness measurement by ellipsometry

Results of the ellipsometric measurement are summarized in Table 2. The thickness of the monolayer measured for deoxo-MA of BCG, and for comparison, those of MeO-MA and Keto-MA from *M. tb* are also shown. Thus the thickness of the monolayer of MeO-MA at $\pi = 30$ mN m^{-1} and $T = 32$ °C is about twice that of MeO-MA at $\pi = 18$ mN m^{-1} and $T = 18$ °C and those of Keto-MA at $\pi = 30$ mN m^{-1} and $T = 18$ °C and $\pi = 20$ mN m^{-1} and $T = 32$ °C. The thickness of MeO-MA monolayer changes from 2.78 nm at $\pi = 18$ mN m^{-1} and $T = 18$ °C, which is almost the same value with the thickness of Keto-MA, drastically to 5.62 nm at $\pi = 30$ mN m^{-1} and $T = 32$ °C. As for Keto-MA whose A^{cp} values imply that its carbonyl group is hydrated at the water surface to give a four-chain molecular conformation, the monolayer thickness is unchanged irrespective of the surface pressure or temperature (Table 2).

The profiles of Langmuir monolayer of deoxo-MA appeared quite different from those of Keto-MA or MeO-MA. As seen in Table 2 even at a low surface pressure such as 4 mN m^{-1}, deoxo-MA molecules apparently seem to be in an extended conformation. When π is scanned at $T = 30$ °C, the monolayer thickness increases by ca. 1 nm as π increases across the phase boundaries.

3.3 Enthalpy changes associated with phase transitions

Enthalpy changes associated with the phase transitions were studied for MeO-MA and deoxo-MA by applying the Clausius-Clapeyron equation derived for insoluble monolayer to their phase diagrams [18].

$$\left(\frac{\partial \pi^{\mathrm{tr}}}{\partial T}\right)_p = \frac{1}{T}\frac{\Delta_l^s h}{\Delta_l^s A}, \tag{1}$$

where

$$\Delta_l^s h = h_{fs} - h_{fl} \tag{2}$$

and

$$\Delta_l^s A = A_{se} - A_{le} \tag{3}$$

and h_{fl} and h_{fs} are the partial molecular enthalpies, and A_{le} and A_{se} are the areas per molecule at equilibrium, in different states. Here, the more condensed state is denoted by 's'. In this work, the A^{tr} and A^{cp} are employed in evaluating $\Delta_l^s A$. They may not be equilibrium values nevertheless it is worth estimating such $\Delta_l^s h$ values. It must be noted that despite the fact that the MA samples employed in this study are not pure substances, we use the equation derived for a monocomponent system since presently it is impossible to obtain pure substances and to experimentally control the molar fractions of the components and at best we treat our systems as pseudo monocomponent ones. Therefore, detailed interpretation of the enthalpy changes of MeO and deoxo-MAs is difficult. Nevertheless, it is important to evaluate $\Delta_l^s h$ values because they are informative of the nature of the phase transition.

Figures 6a and b show enthalpy changes $\Delta_l^s h$ associated with the phase transition shown in Fig. 4 running diagonally from π = 38 to 10 mN m^{-1}

between $T = 10 \sim 32$ °C (—●—) for MeO-MA and the ones at $\pi = 5 \sim 22$ mN m^{-1} and $T = 10 \sim 38$ °C for deoxo-MA, respectively. Additionally, $\Delta_l^s h$ associated with the phase transition observed at around $\pi = 18 \sim 20$ mN m^{-1} between $T = 10 \sim 20$ °C (—△—) in the MeO-MA phase diagram, which involves only a little reorientation of the MA molecules, is evaluated and plotted in Fig. 6a. $\Delta_l^s h$ of the last phase transition takes small negative values. In contrast, the phase transitions which are expected to involve large conformation changes of the meromycolate chain as suggested by the ellipsometric results both for MeO- and Methylene-MA are accompanied by large positive $\Delta_l^s h$ values. In Fig. 4a, the LCI ↔ LCII phase transition line meets the LCI ↔ LCIII and LCII ↔ LCIII transition lines at 21.7 °C. Therefore, in Fig. 6a, $\Delta_l^s h$ vs. T curve corresponding to the phase transitions from the four-hydrocarbon chain to the more extended conformations (—●—) has a break at 21.7 °C and the gap is 5.8 kJ mol^{-1} which is correspondent to the $\Delta_l^s h$ value at 21.7 °C for the LCI ↔ LCII transition (—△—) within the error. Moreover, $\Delta_l^s h$ values of MeO-MA are larger than those of deoxo-MA shown in Fig. 6b at almost all temperatures. The difference is probably partly due to dehydration of the methoxy groups from the water surface. The energy required to break a hydrogen bond is reported to be $17.5 \sim 32.2$ kJ mol^{-1}.

3.4 Computer simulations

MC calculations gave 4-chain structures for all the MAs as illustrated in Figs. 1a and b. The number of the models studied and the results of MD simulation of those models are summarized in Table 3. The Table shows

that by MD simulation of MeO-MA models, more stretched-out structures (Fig. 1c) were obtained than 4-chain structures, whereas by that of Keto-MA, most of the resulting structures were of 4-chain form. The two groups of the torsion angles of the starting models for MC (40 ° group and 92 ° group) apparently did not give different features in MD results.

4 Discussion

4.1 Thermodynamic studies

Langmuir monolayers of the oxygenated MAs from BCG showed complex π vs. A isotherms, as in the case of the MAs from *M. tb* in our previous paper [12]. The isotherms implied that in the lower surface pressure and lower temperature region MeO-MA and deoxo-MA molecules were in 4-chain conformations as Keto-MA but that at the surface pressures above π^{tr}, they were in stretched-out conformations. In contrast, the behavior of deoxo-MA in Langmuir monolayer appears quite different from those of Keto-MA or MeO-MA; even at a low π such as 4 mN m^{-1}, deoxo-MA molecules take an extended conformation. Such conformational features of MeO-, Keto- and deoxo-MAs in Langmuir monolayers suggested by thermodynamic studies were supported by ellipsometric measurement of the thickness of the monolayer.

One possible reason that may explain the difference in the behavior is the difference in the hydrophilic nature of the functional group [X]. The adhesion energy of hydrophilic groups to water surface such as ether, ketone and alcohol groups is said to be fairly independent of other parts of the

molecule and at 20 °C, those of diisopropyl ketone and of diamyl ether are reported to be 74 and 68 mJ m^{-2}, respectively [14]. The difference may not be much, but may play some role in the conformational behaviors of MeO- and Keto-MAs in the water surface monolayers. Deoxo-MA having no hydrophilic group at the [X]-position may be more free to take a stretched-out structure, even at a lower surface pressure.

Enthalpy change associated with phase transition $\Delta_l^s h$ is negative when the transition is from an expanded film to a condensed one with no inter- or intra-molecular interactions involved other than dispersion interaction. Because in the more condensed state, the film forming molecules are closer to each other and energetically more stabilized by the van der Waals attraction than in the expanded state. Therefore, the phase transition becomes exothermic. The phase transition symbolized with —△— in Fig. 4a is such a case and its $\Delta_l^s h$ values are negative as shown in Fig. 6a. On the other hand, when the transition involves dehydration or bond rotations, requiring energy to break hydrogen bonds or to overcome the steric hindrance in revolving C-C bonds, respectively, $\Delta_l^s h$ can become positive. The large positive $\Delta_l^s h$ values in Figs. 6a and b verify that the corresponding phase transitions in Figs. 4a and c are from compact forms to extended ones, involving bond rotations in the meromycolate chains. These phase transitions were implied by the values of average molecular area at the surface pressure of phase transitions and at the collapse pressure and supported by the values of elasticity modulus. Although these data alone may not be a conclusive evidence, the large positive $\Delta_l^s h$ values can be a very strong evidence for the transform of the meromycolate chains from compact folded structures to extended ones.

Additionally, possible involvement of hydration of the methoxy oxygen of MeO-MA in the 4-chain conformation is implied by the difference in $\Delta_l^s h$ observed between MeO-MA and deoxo-MA. The $\Delta_l^s h$ values of MeO-MA are distinctly larger than those of deoxo-MA at almost all temperatures.

4.2 Computer simulations

The structural models of MeO- and Keto-MA produced by MC calculations were all of 4-chain structure. It is interesting that deoxo-MA, whose meromycolate chain had only one functional group, a cyclopropane ring, that might induce chain bending, and had no applied straight-up restrictions in its meromycolate chain, also formed a structure consisting of 4 parallel chain segments [Fig. 1f]. The fact suggests that this type of arrangement of carbon chain segments is appropriate for energetically stable conformations.

As shown in Table 3, after MD simulation, Keto-MA having 4-chain structure normally retained the original 4-chain form [Fig. 1e] and seldom gave stretched-out structures. On the other hand, MeO-MA, whose starting structure is as in Figs. 1a and b, often gave stretched-out structures as shown in Fig. 1c, though some models retained 4-chain structures as seen in Fig. 1d.

Intra-molecular hydrogen bonding involving either the oxo or methoxy group and the 3-hydroxy carboxylic acid group may contribute to some extent to the retaining of the 4-chain structure. However, one of the major causes for the difference observed in the results of MD simulation of the two types of MAs seems to be in the difference in the lengths of the methylene chain segments or in the $n - m - l$ values. As described previously [5], the major component of the MeO-MA from BCG is *cis*-cyclopropyl-containing MeO-

MA acid with the $n-m-l$ value of $17-16-17$, and the minor component with a *trans*-cyclopropane with the $n-m-l$ value of $18-16-17$. In those MeO-MAs, n is larger than m. In the starting models for MD of MeO-MA, having the energetically stabilized 4-chain structure produced by MC (Figs. 1a and b), a bulky group consisting of a methoxy group and the adjacent methyl group is at a position to obstruct the compact arrangement of the 4 chains, as demonstrated by the molecular minimized energy levels: for the models in Table 3, the minimized energy levels of *cis*- and *trans*-MeO-MAs are $-13 \sim -19$ kcal mol^{-1} and $-7 \sim -12$ kcal mol^{-1}, respectively, whereas those of *cis*- and *trans*-Keto-MAs are $-24 \sim -32$ kcal mol^{-1} and $-28 \sim -38$ kcal mol^{-1}. The vibrations of the bulky group locating at or above the location of the 3-hydroxy carboxylate group during MD simulation may disturb the neat arrangement of the neighbouring chains to induce faster and more efficient deviation from the original 4-chain structure. In Keto-MA, the $n-m-l$ value for the major *cis*-cyclopropane containing component is $15-18-17$ or $17-18-17$ and that for the major *trans*-cyclopropane containing component is $16-18-17$, n being smaller than m. Thus, the oxo and the adjacent methyl groups are normally at the end or stretching out of the square pillar-like 4-chain structure. It allows a more compact solid arrangement of the methylene chains in the molecule and the more quiet vibration of the alpha-methyl oxo group may tend to be less disturbing for the 4-chain arrangement during the MD.

The fact that the oxo group is normally situating at the end or out of the 4-chain pillar structure may contribute to the more stable 4-chain structure of Keto-MA in Langmuir monolayers; it assures that the oxo group touches

and bonds to the water surface firmly. On the other hand, in MeO-MA, the methoxy group may often be above the level of the location of the carboxyl group, which touches the water surface. Therefore, although the hydrophilicity of the methoxy group approaches that of an oxo group, the methoxy group may not be able to interact decisively with the water surface.

Deoxo-MAs formed 4-chain-structures with the meromycolate chain bending at the cyclopropane ring and at the methyl branch (Fig. 1f). Probably because they have no bulky functional groups in the vicinity of group [Z] to interact with it, the movement of the structure of deoxo-MA was rather quiet during MD, so that in 20 ps, as shown in Table 3, the structures did not deviate much from the original structure. In fact they often gave more proper 4-chain structures. Easy changes in its conformation observed in the Langmuir monolayers may be due to having no hydrophilic oxo (or methoxy) group and the less well-defined bending capacity of the isolated methyl group. The structure may easily give way when it receives pressure from the neighbouring molecules in the compressed monolayer.

4.3 *Cis* / *trans* stereochemistry.

The possible special influence of MAs with a *trans*-cyclopropane ring on membrane function or pathogenicity of the cells has been highlighted [19,20]. When the features of the Langmuir monolayers of MeO- and Keto-MAs from BCG in the present study were compared with those of the corresponding MAs from *M. tb* in our previous study [12], some differences were noted. The collapse pressures of Keto-MA and the surface pressures of MeO-MA at the phase transition from the 4-chain conformation to the extended one

were lower in those of Keto- and MeO-MAs from BCG, respectively, than in those from *M. tb*, at all the temperatures assayed. The structures of the molecular components of the MAs from the two mycobacteria are essentially identical and the difference is only in the ratios. The ratios between the *cis*-cyclopropane and *trans*-cyclopropane contents are 1/0.03 and 1/0.22, respectively, in MeO-MAs from BCG and *M. tb* and is 1/0.33 and 1/2.7, respectively, in Keto-MAs from BCG and *M. tb*. The differences noted in the respective phase diagrams or isotherms may be attributed to subtle differences in the properties of the *cis*-cyclopropane rings and the *trans*-cyclopropane rings with an adjacent methyl branch. The $\Delta_l^s h$ values corresponding to the changes of four-hydrocarbon chain conformation to a more extended one for *M. tb* MeO-MA are mostly smaller than those for the BCG MeO-MA. Apparently an increased ratio of *trans*-isomers seems to stabilize the four-chain conformation of the oxygenated MAs. The MD studies did not demonstrate any clear difference between the conformational behaviors of *cis*-cyclopropane-containing and *trans*-cyclopropane-containing MAs. This confirms the previous conclusion [12] that *trans*-cyclopropane units, with an adjacent methyl branch, are able to allow folding of MAs in a similar manner to that allowed by *cis*-cyclopropane rings. Further studies on individual molecular species of oxygenated mycolates should be of great value to clear this problem.

Many factors are involved in the process of the onset of infectious diseases. In the case of tuberculosis, the primary and characteristic factor relating to the onset of the disease should be the intrinsic capacity of the *M. tb* cells to resist and reject the attacks by the defense mechanisms of human host

cells. If the mycolate layer of the cell envelope is to play a determining role in the permeability barrier function, as suggested [2,6,9], then the layer is to take an active part in regulating the in and out passages of essential factors vital for the living bacteria and thus to control the viability of the bacterial cells. The component MAs, therefore, may be considered to be responsible for the viability of the *M. tb* cells in human cells and detailed analysis of the physicochemical features of the component MAs may help to clear part of the problems relating to the human tuberculosis.

MAs from pathogenic *M. tb* and from non-pathogenic BCG are the same in the chemical structures of each component and slightly different in the ratios between the *trans*-cyclopropane-containing and *cis*-cyclopropane-containing components. One marked difference between the MAs from the two is in the ratios between the non-oxygenated MA (alpha-MA) and the oxygenated MAs. The ratio in the former is roughly 1:1, whereas that in BCG reaches 1:3.5, in which the oxygenated MA is often mostly Keto-MA [4]. The actual surface pressure in the cell envelope mycolate layer is unknown, but whatever the environmental conditions may be, as demonstrated in the present study, Keto-MAs form compact, relatively solid domains with a minimum thickness in the mycolate monolayer. Such Keto-MA units may provide a relatively impermeable stable foundation in the outer leaflet of the cell envelope. A larger number of, or a larger proportion of this type of less permeable compact domains in BCG cell envelope may provide the cells with the features that distinguish BCG cells from *M. tb* cells. The presence of such solid domains may provide BCG cells with slower and lower multiplication rate and fairly good or moderate resistance to the killing system of the host cells so

that the cells can survive quietly for a long time, which is an essential and necessary requirement for a good live vaccine.

The stretched-out structures of MeO-MA, produced by MD simulation, are not of two long straight methylene chains. As exemplified in Fig. 1c, the long chains curve and bend, implying that they are ready to change their conformation in response to the environmental conditions. Probably MeO-MA and also alpha-MA are to be considered to provide less condensed organelles suitable for facilitating selective permeability and interaction with complex cell surface free lipids.

5 Acknowledgement

This research was supported by Saneyoshi Scholarship Foundation and Mitsubishi Chemical Corporation Fund. D. E. Minnikin is a Leverhulme Emeritus Fellow.

References

[1] M. B. Goren, P. J. Brennan, Mycobacterial lipids: Chemistry and biologic activities; *in* Tuberculosis; G.P. Youmans (ed.) Saunders: Philadelphia, 1979.

[2] D. E. Minnikin, Lipids: Complex Lipids, Their Chemistry, Biosynthesis and Roles; *in* The Biology of the Mycobacteria, Vol. 1. C. Ratledge and J.L. Stanford (eds.) Academic Press: New York, 1982. pp. 95-184.

[3] M. McNeil, M. Daffé, P. J. Brennan, Location of the mycolyl ester substituents in the cell walls of mycobacteria, J. Biol. Chem. 266 (1991) 13217-13223.

[4] M. Watanabe, Y. Aoyagi, M. Ridell, D. E. Minnikin, Separation and characterization of individual mycolic acids in representative mycobacteria, Microbiology 147 (2001) 1825-1837.

[5] M. Watanabe, Y. Aoyagi, H. Mitome, T. Fujita, H. Naoki, M. Ridell, D. E. Minnikin, Location of functional groups in mycobacterial meromycolate chains; the recognition of new structural principles in mycolic acids, Microbiology 148 (2002) 1881-1902.

[6] N. Rastogi, Recent observations concerning structure and function relationships in the mycobacterial cell envelope: elaboration of a model in terms of mycobacterial pathogenicity, virulence and drug-resistance, Res. Microbiol. 142 (1991) 464-476.

[7] X. Hong, A. J. Hopfinger, Construction, molecular modeling, and simulation of *mycobacterium tuberculosis* cell walls, Biomacromolecules 5 (2004) 1052-1065.

[8] M. Jackson, C. Raynaud, M.-A. Lanèelle, C. Guilhot, C. Laurent-Winter, D. Ensergueix, B. Gicquel, M. Daffé, Inactivation of the antigen 85C gene profoundly affects the mycolate content and alters the permeability of the *mycobacterium tuberculosis* cell envelope, Mol. Microbiol. 31 (1999) 1573-1587.

[9] V. Puech, M. Chami, A. Lemassu, M.-A. Lanèelle, B. Schiffler, P. Gounon, N. Bayan, R. Benz, M. Daffé, Structure of the cell envelope of corynebacteria: importance of the non-covalently bound lipids in the formation of the cell wall permeability barrier and fracture plane, Microbiology 147 (2001) 1356-1382.

[10] E. Dubnau, J. Chan, C. Raynaud, V. P. Mohan, M.-A. Lanèelle, K. Yu, A. Quémard, I. Smith, M. Daffée, Oxygenated mycolic acids are necessary for virulence of *Mycobacterium tuberculosis* in mice, Mol. Microbiol. 36 (2000) 630-637.

[11] Y. Yuan, Y. Q. Zhu, D. D. Crane, C. E. Barry III, The effect of oxygenated mycolic acid composition on cell wall function and macrophage growth in *mycobacterium tuberculosis*, Mol. Microbiol. 29 (1998) 1449-1458.

[12] M. Villeneuve, M. Kawai, H. Kanashima, M. Watanabe, D. E. Minnikin, H. Nakahara, Temperature dependence of the Langmuir monolayer packing of mycolic acids from *Mycobacterium tuberculosis*, Biochim. Biophys. Acta 1715 (2005) 71-80.

[13] A. Dupré, *in* Théorie mécanique de la chaleur p. 207, Paris 1869.

[14] C. O. Timmons, W. A. Zisman, The relation of initial spreading pressure of polar compounds on water to interfacial tension, work of adhesion, and solubility, J.C.I.S. 28 (1968) 106-117.

[15] S. C. Macave, M.-A. Lanèelle, M. Daffé, H. Montrozier, M. P. Pols, C. Asselineau, Étude structurale et métabolique des acides mycoliques de *Mycobacterium fortuitum*, Eur. J. Biochem. 163 (1987) 369-378.

[16] K. G. R. Pachler, The dependence of vicinal proton-proton coupling constants on dihedral angles and substituents, J. Chem. Soc. Perkin II (1972) 1936-1939.

[17] C. A. G. Haasnoot, F. A. A. M. de Leeuw, C. Altona, The relationship between proton-proton NMR coupling constants and substituent electronegativities-I. An empirical generalization of the Karplus equation, Tetrahedron 36 (1980) 2783-2792.

[18] K. Motomura, Thermodynamics and phase transitions in monolayers, J.C.I.S. 23 (1967) 313-318.

[19] M. S. Glickman, J. S. Cox, W. R. Jacobs, Jr., A novel mycolic acid cyclopropane synthetase is required for cording, persistence and virulence of *Mycobacterium tuberculosis*, Mol. Cell 5 (2000) 717-727.

[20] M. S. Glickman, S. M. Cahill, W. R. Jacobs, Jr., The *Mycobacterium tuberculosis cmaA2* gene encodes a mycolic acid *trans*-cyclopropane synthetase, J. Biol. Chem. 276 (2001) 2228-2233.

FIGURE LEGENDS

Fig. 1. Structures of MAs in MD study. (a) and (b) Top and side views of MeO-MA molecule obtained by MC followed by minimization; (c) MeO-MA taking a stretched-out structure after 20 ps in MD; (d) MeO-MA retaining a 4-cain structure after 20 ps in MD; (e) structure of Keto-MA obtained after 20 ps in MD; (f) structure of deoxo-MA obtained by MC followed by minimization.

Fig. 2a. General structure of MA. Fat lines refer to the methylene chain segments in which the carbon torsion angles were set to 180 degrees for Monte Carlo calculation. Three carbons on both sides of [X] and of [Y], and two carbons on both sides of [Z] were not included in the restricted portions. For MC of deoxo-MA, the restriction was not applied to its meromycolate chain.

Fig. 2b. General structure of *trans*-cyclopropyl group-containing Keto-MA to illustrate the points used for evaluation of the results of MD simulation study. a) End carbon of 2-alkyl chain; b) carboxyl group-bearing carbon; c) distal carbon of cyclopropane ring; d) oxo group-bearing carbon (in MeO-MA, methoxy group-bearing carbon and in deoxo-MA, methylene-carbon next to the methyl side chain; e) distal end carbon of meromycolate chain.

Fig. 3. Surface pressure vs. mean molecular area isotherms of mycolic acids. Not all the isotherms are shown. (a) MeO-MA; (b) Keto-MA; (c) deoxo-MA. Figures in the graphs refer to the temperatures at which the measurement was performed. In (a), 1 to 9 refer to temperatures 10, 14, 18, 22, 26, 32, 36, 42, and 46 °C, respectively; in (b), 1-11 refer to the temperatures 10, 14, 18, 22, 26, 28, 32, 34, 38, 42, and 46 °C, respectively; and in (c), 1-10 refer to the temperatures 10, 14, 18, 22, 26, 30, 34, 38, 42

and 46 °C, respectively.

Fig. 4. Phase diagrams of Langmuir monolayers: (—●—), (—△—), (—□—) or (—■—) π^{tr} vs. T; (—◯—) π^{cp} vs. T curves; SC refers to the solid condensed state, LC to the liquid condensed state, LE to the liquid expanded state. (a) MeO-MA; (b) Keto-MA: (c) deoxo-MA.

Fig. 5. Mean molecular area at the phase transition pressure A^{tr} vs. temperature T (●, △, □ or ■; the symbols correspond to the phase transitions indicated in Fig. 3) and mean molecular area at the collapse pressure A^{cp} vs. T (◯). (a) MeO-MA; (b) Keto-MA; (c) deoxo-MA.

Fig. 6. Enthalpy changes associated with phase transition $\Delta_l^s h$ vs. T. The symbols correspond to the phase transitions indicated in Fig. 3. (a) MeO-MA from BCG, △ refers to $\Delta_l^s h$ associated with the phase transition from a four-chain conformation to another four-chain one; ● to $\Delta_l^s h$ from a four-chain conformation to an extended one; (b) deoxo-MA, □ and ■ refer to $\Delta_l^s h$ associated with the phase transitions between different conformations; (c) MeO-MA from *M. tb*, $\Delta_l^s h$ associated with the phase transition from a four-chain conformation to an extended one.

Table 1. Structures, compositions and average molecular weights of MAs from *M. bovis* BCG.

CH_3-$(CH_2)_l$-[X]-$(CH_2)_m$-[Y]-$(CH_2)_n$-CH(OH)-CH(COOH)-$(CH_2)_{23}$-CH_3

Samples	Distal group [X]	Proximal group [Y]	*n-m-l* [1]	*cis/trans* [2]	Av. MW
MeO-MA	-$CH(CH_3)$-$CH(OCH_3)$-	*cis* -cyclopropane	17-16-17	1/0.03	1252
		trans -cyclopropane	18-16-17		
Keto-MA	-$CH(CH_3)$-CO-	*cis* -cyclopropane	15-18-17	1/0.33	1246
		cis -cyclopropane	17-18-17		
		trans -cyclopropane	16-18-17		
Deoxo-MA	-$CH(CH_3)$-CH_2-	*cis* -cyclopropane	15-18-17	1/0.33 [3]	1232
		cis -cyclopropane	17-18-17		
		trans -cyclopropane	16-18-17		

1) Values of major components.

2) Ratios implied by ^{1}H-NMR spectra.

3) Ratio assumed to be the same as that of parent Keto-MA.

Table 2. Thickness of Langmuir monolayer estimated by ellipsometry.

origin	Keto-MA		MeO-MA		Deoxo-MA	
	T/°C π/mN m^{-1}	thickness/nm	T/°C π/mN m^{-1}	thickness/nm	T/°C π/mN m^{-1}	thickness/nm
BCG	18 30	2.90±0.05	18 18	2.78±0.04	30 4	3.98±0.09
	32 20	2.80±0.08	32 30	5.62±0.18	30 20	4.81±0.11
					30 40	6.10±0.08
M. tb	18 30	2.90±0.07	18 18	2.91±0.05		
			32 30	4.96±0.88		

Table 3. Results of computer simulations.

Methoxymycolic acid

Cyclo-propane	*n-m-l*	Torsion angle [1]	No. of models for MC	No. of models for MD	Conformations defined [2] A	Conformations defined [2] B	Conformations defined [2] A/B	Undefinable structure
cis	17-16-17	40	4	18	7	7[3]	1	3
		92	3	15	5	5	2	3
trans	18-16-17	40	2	10	3	6	1	
		92	2	9	3	5[3]		1

Ketomycolic acid

Cyclo-propane	*n-m-l*	Torsion angle [1]	No. of models for MC	No. of models for MD	Conformations defined [2] A	Conformations defined [2] B	Conformations defined [2] A/B	Undefinable structure
cis	15-18-17	40	4	20	12[3]	1	2	5
		92	3	13	12			1
cis	17-18-17	40	3	14	10		1	3
		92	2	10	4		1	5
trans	16-18-17	40	1	4	4			
		92	3	12	9		1	2

Deoxomycolic acid

Cyclo-propane	*n-m-l*	Torsion angle [1]	No. of models for MC	No. of models for MD	Conformations defined [2] A	Conformations defined [2] B	Conformations defined [2] A/B	Undefinable structure
cis	17-18-17	40	1	6	4		1	1
		92	2	10	7			3

1) Torsion angles in degrees, involving carbons 2 and 3 and the two adjacent carbons on either side in [Z] in Fig. 2a. 40 and 92 include the set angles at start of 40 and 41 degrees and 92, 93 and 94 degrees, respectively.

2) For definition of each conformation, please refer to the text. A: four-chain structure, B: stretched-out structure, A/B: between A and B.

3) Each contains one member in which the distal end tip of the chain a/b is bent.

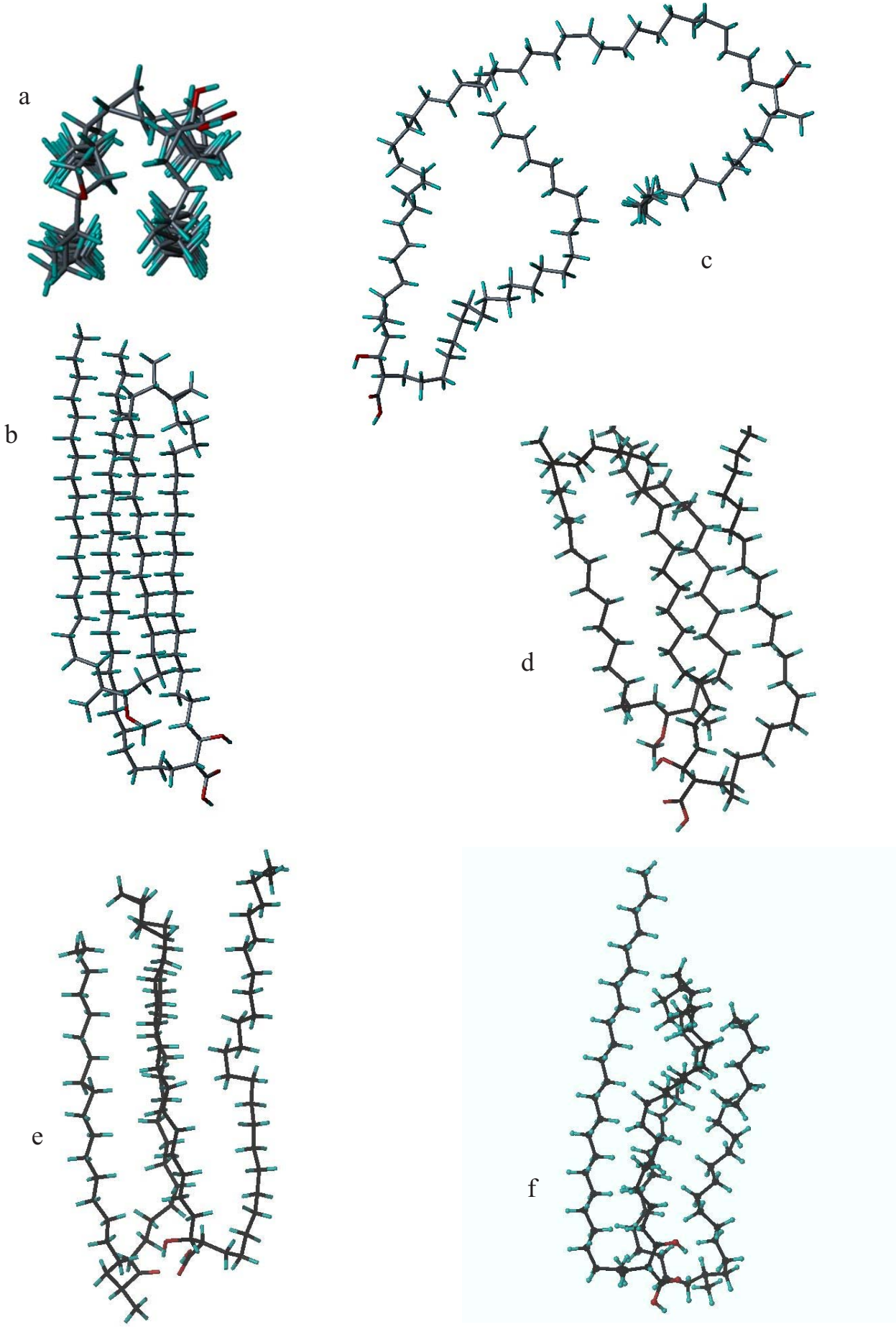

Fig. 1 Villeneuve et al.

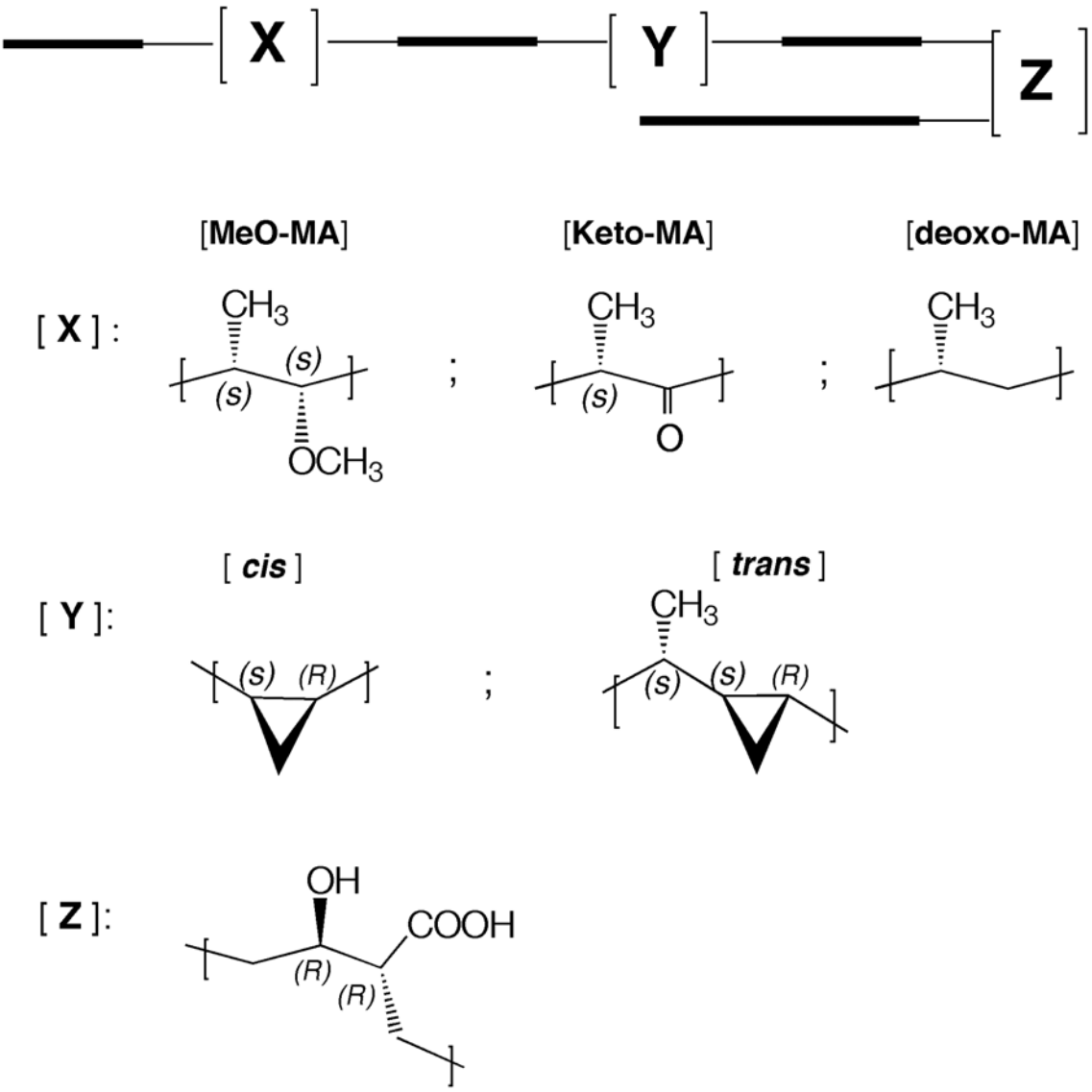

Figure 2a

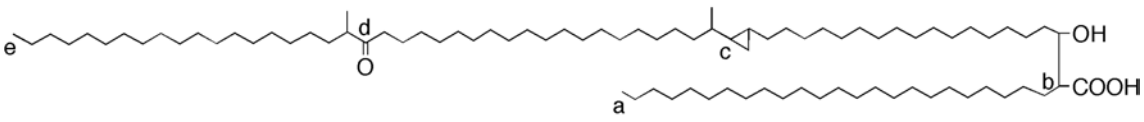

Figure 2b

Fig.2 Villeneuve et al.

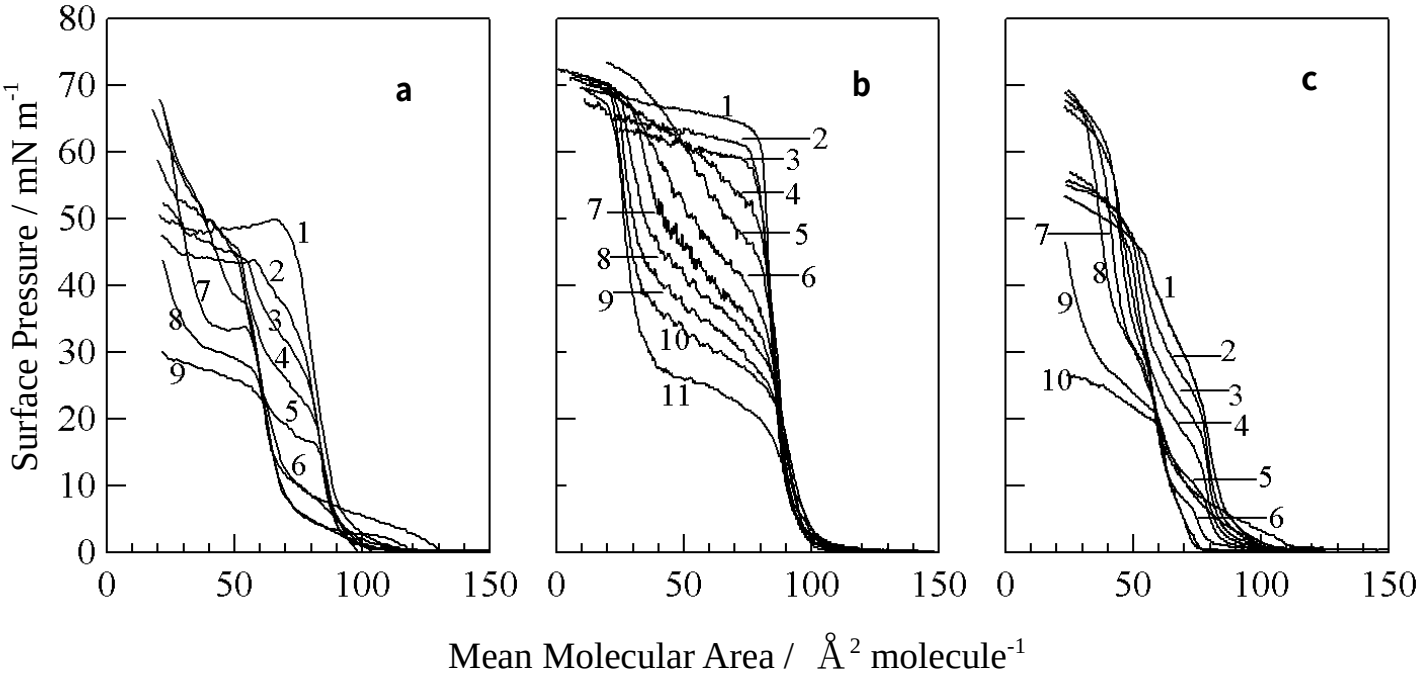

Fig. 3 Villeneuve et al.

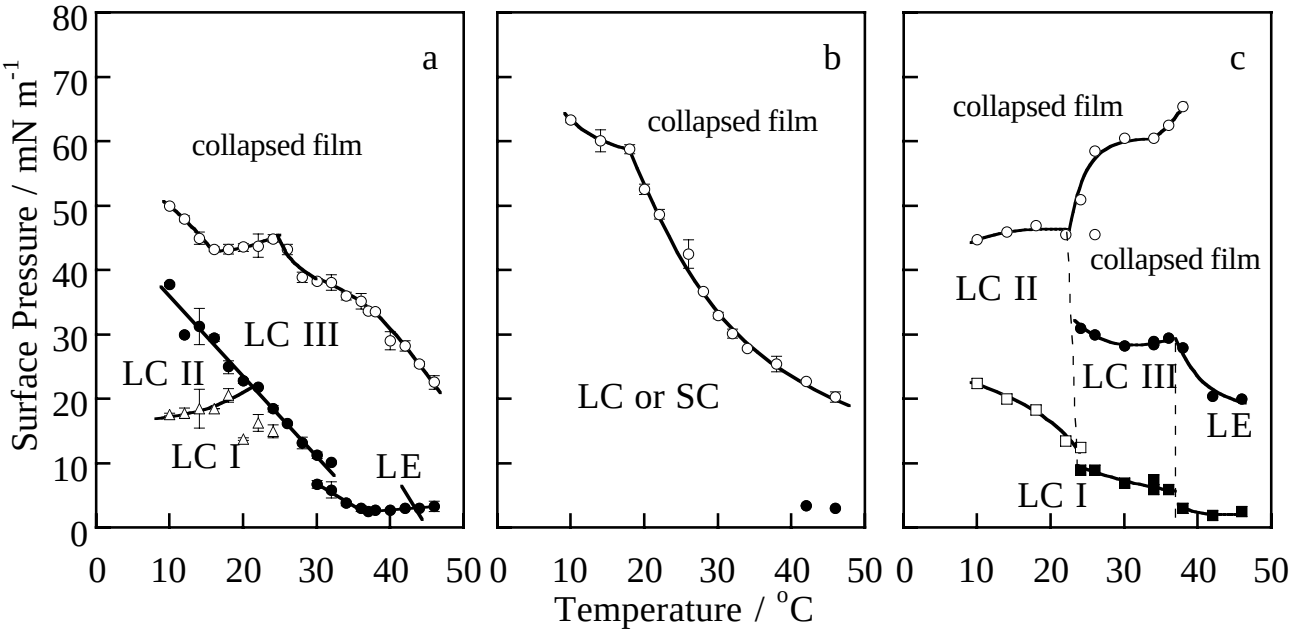

Fig. 4 Villeneuve et al.

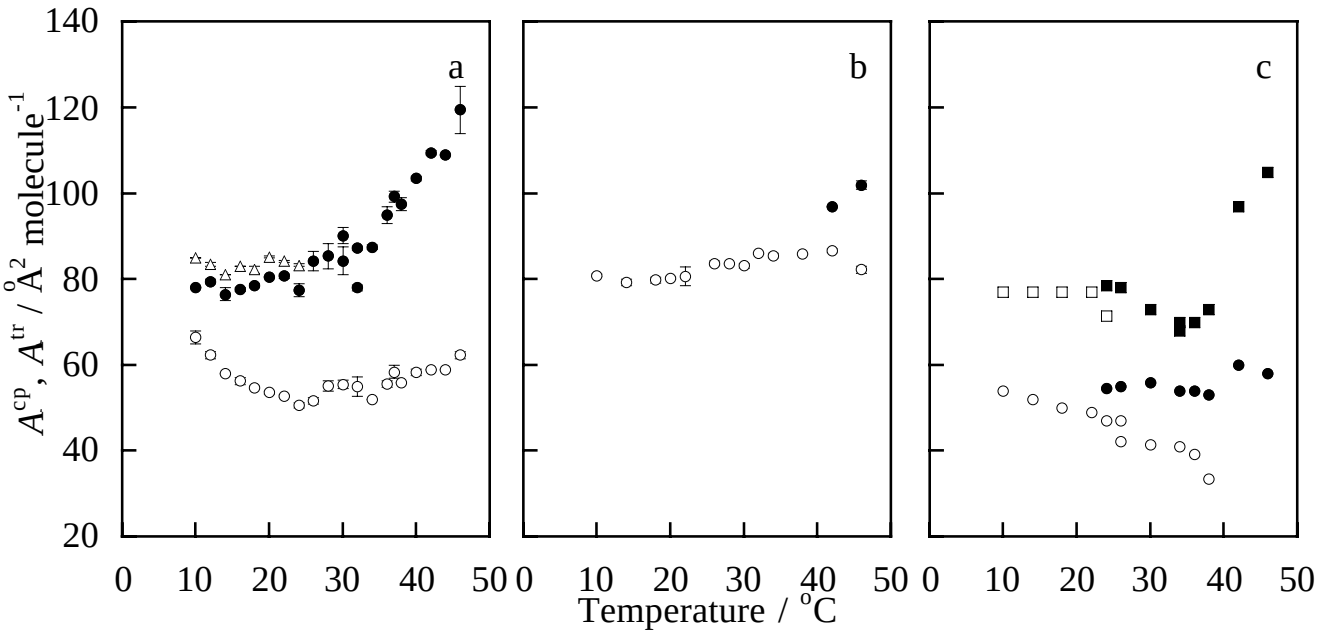

Fig. 5 Villeneuve et al.

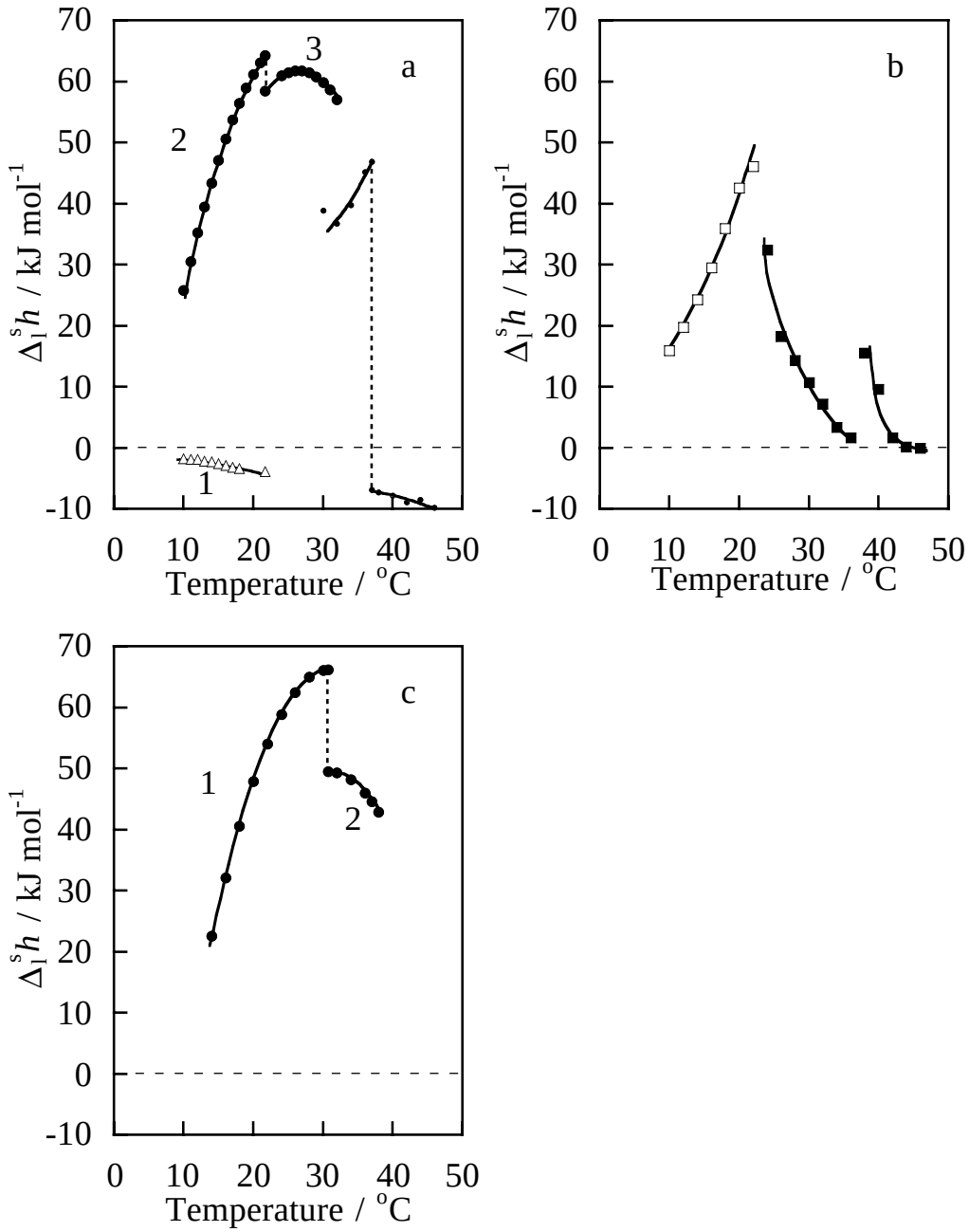

Fig. 6 Villeneuve et al.